Spironolactone and Its Main Metabolite, Canrenoic Acid, Block Human Ether-a-Go-Go–Related Gene Channels

Ricardo Caballero, Ignacio Moreno, Teresa González, Cristina Arias, Carmen Valenzuela, Eva Delpón and Juan Tamargo

Circulation 2003;107;889-895; originally published online Feb 3, 2003;
DOI: 10.1161/01.CIR.0000048189.58449.F7
Circulation is published by the American Heart Association. 7272 Greenville Avenue, Dallas, TX 72514
 Print ISSN: 0009-7322. Online ISSN: 1524-4539

Spironolactone and Its Main Metabolite, Canrenoic Acid, Block Human Ether-a-Go-Go–Related Gene Channels

Ricardo Caballero, BPharm, PhD*; Ignacio Moreno, BPharm*; Teresa González, BSc; Cristina Arias, BSc; Carmen Valenzuela, BSc, PhD; Eva Delpón, BPharm, PhD; Juan Tamargo, MD, PhD, FESC

Background—It has been demonstrated that spironolactone (SP) decreases the QT dispersion in chronic heart failure. In this study, the effects of SP and its metabolite, canrenoic acid (CA), on human ether-a-go-go–related gene (HERG) currents were analyzed.

Methods and Results—HERG currents elicited in stably transfected Chinese hamster ovary cells were measured with the whole-cell patch-clamp technique. SP decreased HERG currents in a concentration-dependent manner (IC_{50}=23.0±1.5 μmol/L) and shifted the midpoint of the activation curve to more negative potentials (Vh=−13.1±3.4 versus −18.9±3.6 mV, $P<0.05$) without modifying the activation and deactivation kinetics. SP-induced block (1 μmol/L) appeared at the range of membrane potentials coinciding with that of channel activation, and thereafter, it remained constant, reaching 24.7±3.8% at +60 mV (n=6, $P<0.05$). CA (0.01 nmol/L to 500 μmol/L) blocked HERG channels in a voltage- and frequency-independent manner. CA at 1 nmol/L shifted the midpoint of the activation curve to −19.9±1.8 mV and accelerated the time course of channel activation (τ=1064±125 versus 820±93 ms, n=11, $P<0.01$). The envelope of the tail test demonstrated that at the very beginning of the pulses to +40 mV (25 ms), a certain amount of block was apparent (31.3±9.9%). CA did not modify the voltage-dependence of HERG channel inactivation (Vh=−60.8±5.6 versus −62.9±3.1 mV, n=6, $P>0.05$) or the kinetics of the reactivation process at any potential tested. CA and aldosterone also blocked the native I_{Kr} in guinea-pig ventricular myocytes.

Conclusions—At concentrations reached after administration of therapeutic doses of SP, CA blocked the HERG channels by binding to both the closed and open states of the channel. **(*Circulation*. 2003;107:889-895.)**

Key Words: ion channels ■ potassium channels ■ patch-clamp techniques ■ spironolactone

Spironolactone (SP) is an aldosterone antagonist used in the treatment of hypertension, congestive heart failure, and cirrhotic ascites.[1] In patients with advanced heart failure, the Randomized Aldactone Evaluation Study (RALES) showed that the addition of low-dose SP to an ACE inhibitor and a loop diuretic improved survival.[2] Furthermore, SP reduced heart rate and improved heart rate variability and QT dispersion in chronic heart failure.[3] This latter result was empirically attributed to the antagonism of the proarrhythmic effects of aldosterone at the receptor level. In fact, aldosterone causes sodium retention, myocardial fibrosis, and potassium and magnesium depletion; potentiates the effects of catecholamines; blunts the baroreflex response; and induces ventricular arrhythmias.[4]

SP is extensively metabolized in humans, and ≈79% of the SP oral dose is converted to canrenone, its major biologically active metabolite.[5] Canrenone undergoes hydrolysis of its γ-lactone ring to canrenoic acid (CA), which is water soluble. Thus, after equilibrium, similar plasma concentrations of CA and canrenone are reached. Two old studies demonstrated that SP lengthened the duration and refractoriness of the cardiac action potential,[6,7] effects that were attributed to a decrease in K^+ conductance but that were not investigated further.[7] Thus, the effects of SP and CA on cardiac K^+ channels are currently unknown. Because the rapid component of the delayed rectifier K^+ current (I_{Kr}) carried by human ether-a-go-go–related gene (HERG) channels plays a critical role in the control of the action potential repolarization in humans,[8] the present study was undertaken to test whether SP and CA modify HERG channels cloned from human heart and stably expressed in a mammalian cell line.

Methods

Stably transfected CHO cells were cultured as previously described[9,10] and perfused with an external solution containing (in mmol/L): NaCl 130, KCl 4, $CaCl_2$ 1, $MgCl_2$ 1, HEPES 10, and glucose 10 (pH adjusted to 7.4 with NaOH). The internal solution contained (in mmol/L): K-aspartate 80, KCl 42, KH_2PO_4 10, MgATP 5, phosphocreatine 3, HEPES 5, and EGTA 5 (pH adjusted to 7.2

Received July 30, 2002; revision received October 30, 2002; accepted October 30, 2002.

From the Department of Pharmacology, School of Medicine, Universidad Complutense, Madrid, Spain.

*The first 2 authors contributed equally to this work.

Correspondence to Eva Delpón, Department of Pharmacology, School of Medicine, Universidad Complutense, 28040 Madrid, Spain. E-mail edelpon@med.ucm.es

Circulation **is available at http://www.circulationaha.org** **DOI: 10.1161/01.CIR.0000048189.58449.F7**

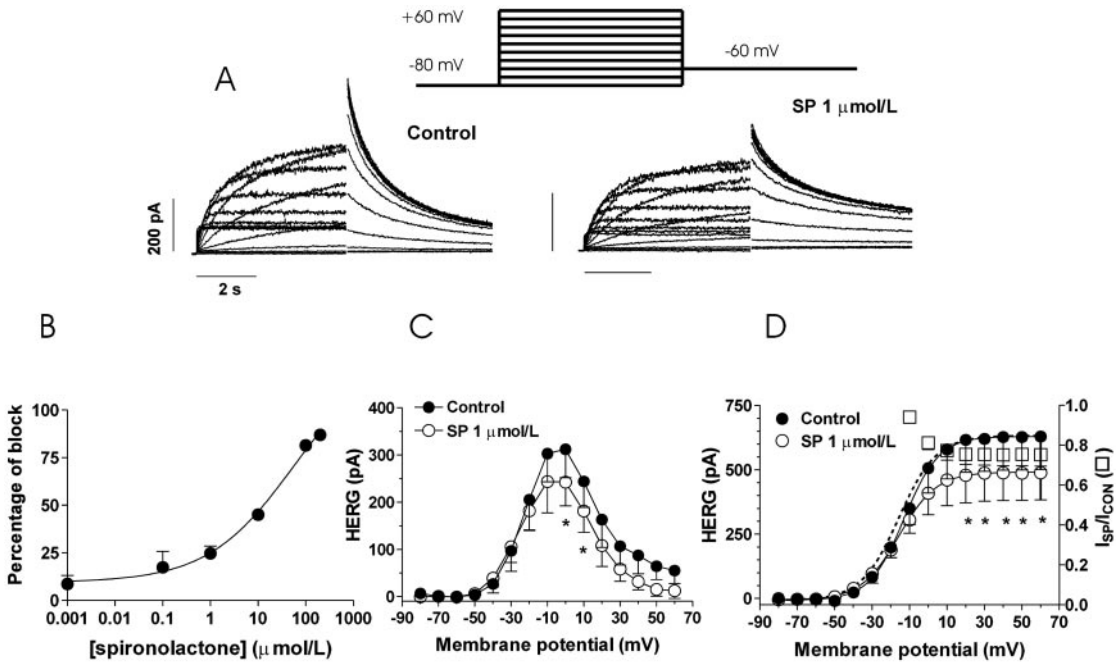

Figure 1. A, Current traces obtained with voltage protocol illustrated at top for control conditions and with 1 μmol/L SP. B, Concentration-response relation for block of HERG tail currents elicited on repolarization to −60 mV after 5-second pulses to +60 mV. Continuous line represents fit of data to Hill equation. Each point represents mean±SEM of >4 experiments. C, Averaged current-voltage relationship 5-second isochronal in absence and in presence of SP. D, Averaged activation curves as calculated from peak tail-current amplitudes under control and SP. Dashed line represents normalized activation curve in presence of SP. Squares represent fractional tail-current block as a function of membrane potential. C and D, points represent mean±SEM of 6 experiments. *$P<0.05$ vs control.

with KOH). Guinea pig ventricular myocytes were enzymatically isolated and perfused with the same external solution supplemented with 2 mmol/L $CoCl_2$ and 30 μmol/L tetrodotoxin.[10] SP and CA (Sigma) were dissolved in dimethyl sulfoxide and methanol, respectively, to make 10 mmol/L stock solution.

HERG and I_K currents were measured by use of the whole-cell and the perforated-nystatin configurations of the patch-clamp technique, respectively.[10] Recordings were performed at 24°C to 25°C with 200B patch-clamp amplifiers. Capacitance and series resistance compensation were optimized, and ≈80% compensation was usually obtained. Maximum HERG tail-current amplitudes averaged 520±75 pA, mean uncompensated access resistance was 4.5±0.3 MΩ, and cell capacitance was 14.9±0.7 pF (n=22). In ventricular myocytes, the effective access resistance averaged 12.8±0.9 MΩ and the larger current amplitude 260±45 pA (n=6). Thus, no significant voltage errors (<5 mV) were expected with the electrodes used (tip resistance <3 MΩ). The inhibitory concentration at which 50% of block was achieved, IC_{50}, and Hill coefficient, n_H, were obtained from fitting the fractional block, f, at various drug concentrations [D] to the Hill equation:

$$f=1/\{1+(IC_{50}/[D])^{nH}\}.$$

Results are expressed as mean±SEM. Data were compared by ANOVA followed by the Newman-Keuls test. A value of $P<0.05$ was considered significant.

Results

Concentration-Dependent Effects of SP and CA

Figure 1 summarizes the effects of 1 μmol/L SP on HERG currents. Families of current traces are shown for control conditions and after 10 minutes of exposure to SP obtained by applying 5-second pulses to voltages between −80 and +60 mV in 10 mV increments (A). The holding potential was fixed at −80 mV, and tail currents were recorded on repolarization to −60 mV for 5 seconds. SP decreased both the outward and the tail currents and accelerated the time course of channel activation measured from the exponential fits of the current traces elicited at 0 mV (Table). Furthermore, SP did not modify the decline of tail currents elicited

Effects of SP and CA on the Characteristics of HERG Currents

	Control	SP, 1 μmol/L	Control	CA, 1 nmol/L
Vh (activation), mV	−13.1±3.4	−18.9±3.6*	−17.1±2.3	−19.9±1.8*
k (activation), mV	8.4±0.2	8.9±0.4	8.7±0.5	8.9±0.6
$\tau_{activation}$, ms	1354±215	998±170*	1064±125	820±93*
$\tau f_{deactivation}$, ms	308.4±26.4	364.2±39.6	323.9±34.5	470.1±45.6*
$\tau s_{deactivation}$, ms	1470±95	1752±226	1833±255	2196±270*

Data are mean±SEM of 6 and 11 experiments in the presence of SP and CA, respectively.
*$P<0.05$ vs control.

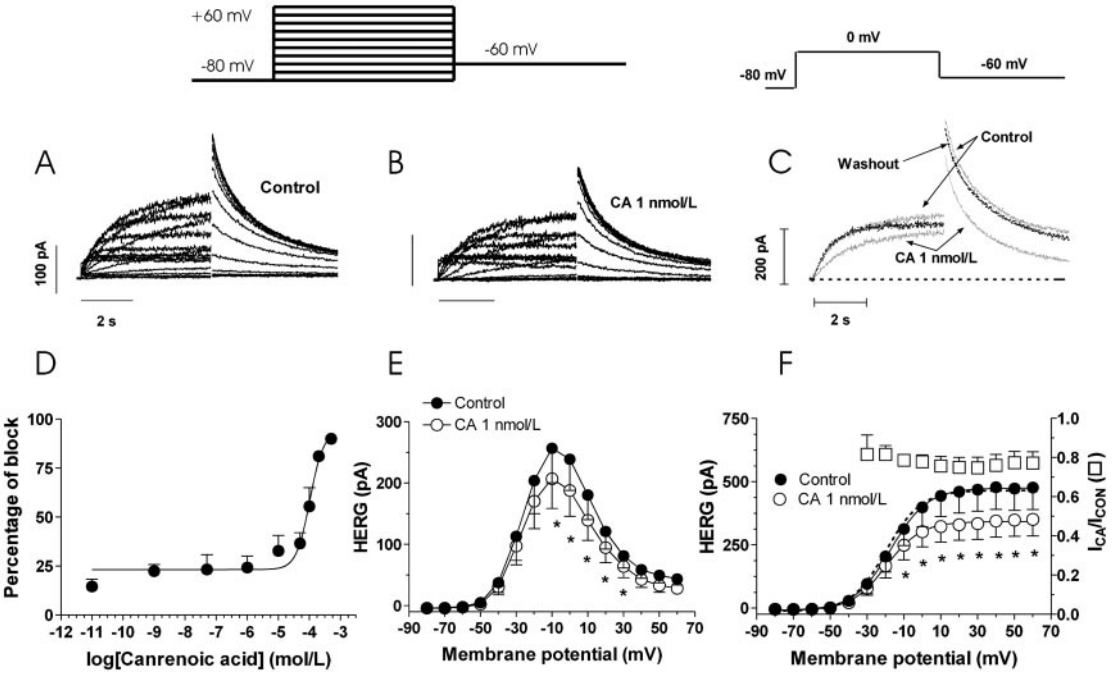

Figure 2. A, Current traces obtained with voltage protocol illustrated at top for control conditions and with CA (B). C, Superimposed current traces obtained in absence and in presence of CA and after washout with drug-free solution. D, Concentration-response relationship for block of HERG tail currents elicited on repolarization to −60 mV after 5-second pulses to +60 mV. Continuous line represents fit of data to Hill equation. Each point represents mean±SEM of >5 experiments. E, Averaged current-voltage relationship 5-second isochronal in absence and in presence of CA. F, Averaged activation curves as calculated from peak tail-current amplitudes under control and CA. Dashed line represents normalized activation curve in presence of CA. Squares represent fractional tail-current block as a function of membrane potential. E and F, Points represent mean±SEM of 11 experiments. *$P<0.05$ vs control.

on repolarization to −60 mV after pulses to +60 mV, and thus, both the fast (τ_f) and the slow (τ_s) time constants of deactivation remained unaltered (Table). The concentration-dependence of the blockade measured on the peak tail current elicited on repolarization after pulses to +60 mV was fitted to the Hill equation and yielded an IC_{50} of 23.0±1.5 μmol/L (n_H=0.8±0). Current-voltage plots of steady-state current present at the end of the depolarizing step (current-voltage relationship) and peak tail current (activation curve) are depicted in Figure 1, C and D, respectively. In the presence of SP, steady-state current amplitude elicited at 0 mV was reduced by 18.9±4.2% (n=6, $P<0.05$). In 6 cells, SP shifted the midpoint of the activation curve (D, continuous lines) to more negative potentials but did not modify the slope factor (Table). The squares in D represent the fractional tail-current block as a function of the membrane potential. The results indicated that blockade appeared at the range of membrane potentials coinciding with that at which channel activation occurred, and thereafter it remained constant, reaching 24.7±3.8% at +60 mV (n=6, $P<0.05$).

Figure 2, A and B, shows current traces obtained in the absence and in the presence, respectively, of 1 nmol/L CA. CA also decreased both the outward and the tail HERG currents, and these effects were almost completely reversed after washout (Figure 2C). Figure 2D shows the extent of block of tail currents elicited on repolarization after pulses to +60 mV by CA (concentration-response curve). Surprisingly, the percentage of tail-current block remained almost constant for concentrations ranging from 0.01 nmol/L to 1 μmol/L, and thereafter, it increased as the concentration of CA was increased. The IC_{50} and the n_H obtained by fitting the Hill equation to the data averaged 104.3±1.2 μmol/L and 1.9±0.6, respectively. To analyze the frequency-, time-, and voltage-dependence of CA-induced block, the concentration of 1 nmol/L was selected. CA decreased the current amplitude at potentials ranging from −10 to +30 mV, reaching 22.7±1.5% of block at 0 mV (n=11, $P<0.05$). CA also decreased the tail-current amplitude recorded on repolarization to −60 mV (Figure 2F) and shifted the midpoint of the activation curve toward more negative potentials without modifying the slope factor (Table). In F, the squares represent the fractional tail-current block as a function of the membrane potential. The blockade was already apparent before channel activation reached saturation, and it remained constant in a wide range of potentials, averaging 18.3±4.5% and 22.7±5.7% at −30 and +60 mV, respectively (n=11, $P>0.05$).

To analyze whether the CA-induced block was frequency-dependent, trains of 200-ms pulses to +60 mV at 1 or 2 Hz were applied in 2 different groups of cells (Figure 3, A and B). Under control conditions, the tail-current amplitude remained unchanged both at 1 and at 2 Hz, and CA-induced block was almost fully developed with the first pulse of the train. C represents the ratio of the tail-current amplitude as a function of the number of pulses during the train. CA decreased the tail amplitude of the first and the last pulse of trains at 1 and 2 Hz to a similar extent, which indicated that CA did not produce a frequency-dependent block of HERG channels.

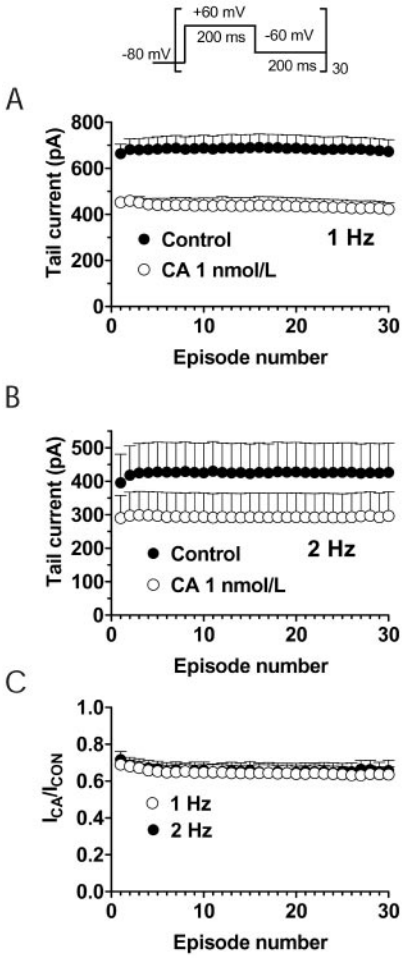

Figure 3. Voltage-clamp pulse trains (protocol shown in inset) were applied at (A) 1 and (B) 2 Hz. Mean tail-current amplitude in absence and in presence of 1 nmol/L CA were plotted vs pulse number. C, Ratio of tail-current amplitudes in absence and presence of CA as a function of pulse number.

Time-Dependent Inhibition by CA

Time-dependent inhibition of HERG channels by CA was first measured by use of an envelope of tail test (Figure 4, A and B). Tail currents were generated on repolarization to −60 mV after application of voltage steps of increasing duration to +40 mV. Both in the absence and in the presence of CA tail current amplitudes increased in a monoexponential fashion as the pulse was lengthened ($\tau_{Control}$=192.9±11.2 and τ_{CA}=122.2±8.5 ms; n=11, $P<0.05$). Fractional block as a function of the pulse duration is shown in Figure 4, C and D. The results suggested that at the beginning of the depolarization, a certain amount of block was apparent (31.3±9.9%), which decreased within the first 100 ms (18.3±6.8%; n=6, $P>0.05$). Thereafter, the blockade slightly increased with the depolarization, but this increase did not reach statistical significance. The onset of the CA-induced block was well fitted with a single exponential function, and the τ_{block} averaged 349±102 ms (n=6).

Figure 4E shows superimposed current traces obtained by use of a protocol previously described by Zhang et al.[11] We analyzed the development of block during a 200-ms pulse to 0 mV preceded by a 5-ms depolarization to +180 mV. Under these conditions, the current at 0 mV was nearly constant, and tail current was recorded with the subsequent repolarizing step to −60 mV. Once again, virtually all of the final effect of CA was already present at the beginning of the step, ie, CA simply scaled down the current at 0 mV and the tail current by 17.3±1.5% and 20.6±1.9%, respectively (n=6, $P>0.05$).

The time-dependence of the CA-induced block was also studied from the exponential fits of the current traces elicited at 0 mV, and the results demonstrated that CA accelerated the time course of current activation (Table). Deactivation kinetics of tail currents elicited on return to −60 mV after pulses to +60 mV was slowed in the presence of CA (Table). In contrast, deactivation kinetics of tail currents after pulses to 0 mV was not modified. In fact, both the fast and the slow time constants of deactivation in the absence (τ_f=315.9±32.6 and τ_s=1808±118 ms) and the presence (τ_f=342.2±23.1 and τ_s=1853±137 ms) of CA remained unaltered (n=11, $P>0.05$). Figure 4F shows the ratio of tail currents elicited on return to −60 mV after pulses to 0 mV. Within the first second of repolarization, the blockade increased slightly, and thereafter it decreased progressively. The time-dependent effects of CA suggested that it blocked HERG channels in the closed and in the open state.

Effects of CA on the Inactivation and Reactivation of HERG Channels

We next looked for changes in the steady-state inactivation (availability) of the channels. The protocol used is described in Figure 5A, together with typical current records obtained in the absence of CA. After a 1-second pulse to +40 mV to activate the channels, the membrane voltage was stepped briefly to various test voltages and then to +40 mV. During the brief step, the inactivation process relaxed rapidly to the steady-state level appropriate to the test potential. The initial current on stepping to +40 mV gave the relative number of open channels. Figure 5B represents the initial current amplitude at +40 mV (arrow in A) against the interpulse potential. At negative voltages, the currents decline because significant closing of channels occurred through deactivation. Thus, in Figure 5C, this was corrected for by extrapolating the exponential falling phase back to the start of the negative voltage step and applying the same relative correction to the initial outward current. This procedure was described previously for the same purpose.[12] The Vh of the corrected for closing, and the uncorrected inactivation curves averaged −60.8±5.6 mV (k=21.1±1.5 mV) and −49.9±3.0 mV (k=16.3±1.8 mV), respectively. CA did not modify the voltage-dependence of HERG channel inactivation; thus, the Vh of the corrected-for closing inactivation curves averaged −62.9±3.1 mV (k=21.6±1.9 mV; n=6, $P>0.05$), whereas that of the uncorrected averaged −51.7±1.9 mV (k=16.5±1.9; n=6, $P>0.05$). Figure 5D represents the fractional block as a function of the interpulse potential and indicated that the blockade was not significantly modified by the channel inactivation.

To assess whether CA altered the recovery from inactivation, a protocol similar to that of Spector et al[13] was used. The membrane was repolarized 100 ms to voltages ranging from

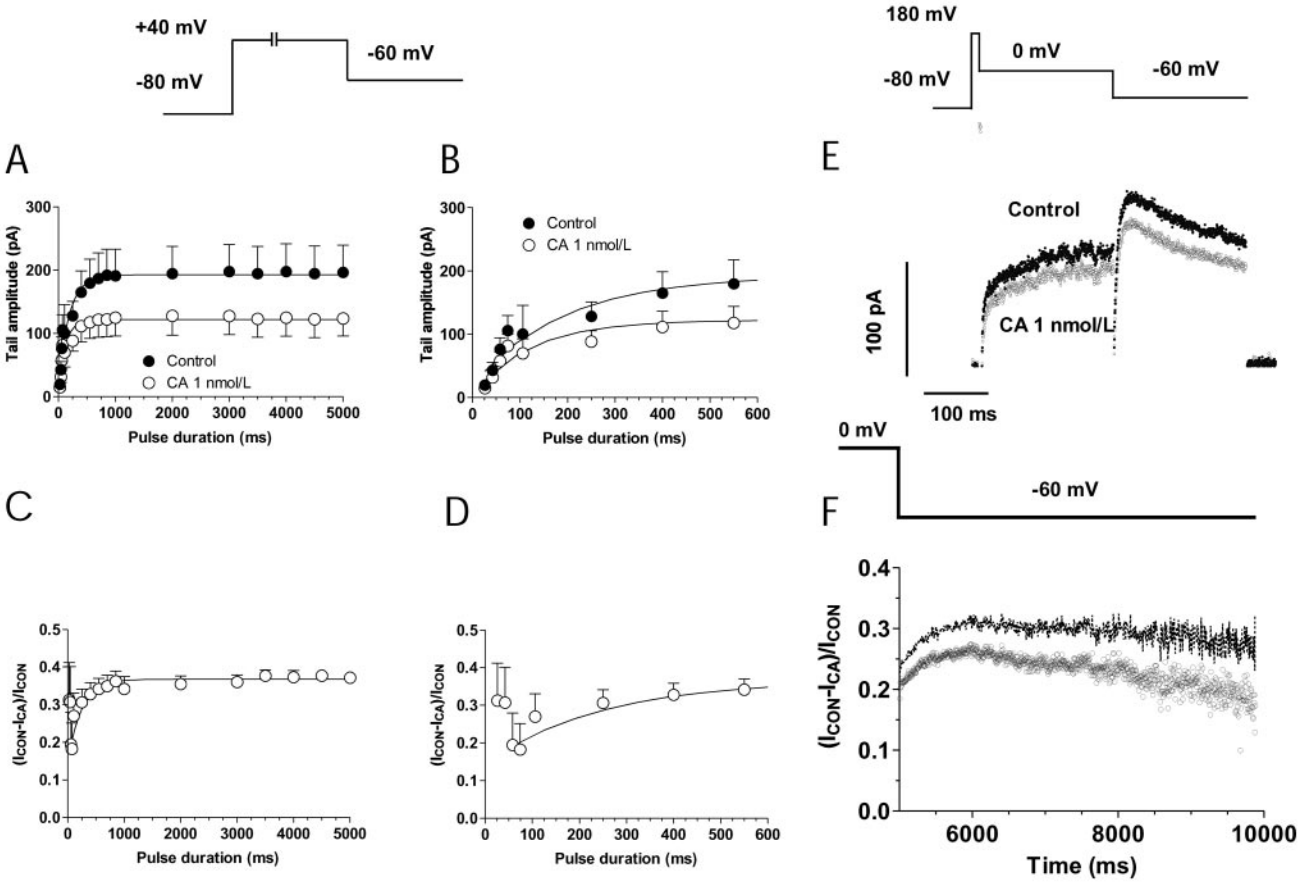

Figure 4. Envelope of tail-current test under control conditions and with 1 nmol/L CA. Pulses to +40 mV of increasing duration (25 ms to 5 seconds) were applied every 30 seconds. Peak tail current after return to −60 mV was plotted as a function of test pulse duration in A. Continuous lines represent monoexponential that fits experimental data. B, Expanded time scale of data presented in A. C, Fractional tail-current block produced by CA as a function of test pulse duration. Continuous line represents monoexponential that fits experimental data. D, Expanded time scale of data presented in C. A through D, Points represent mean±SEM of 6 experiments. E, Superimposed current traces in control conditions and in presence of CA are shown. HERG current was rapidly activated from a holding potential of −80 mV by a 5-ms step to +180 mV followed by a step to 0 mV. Tail currents were observed on repolarization to −60 mV. F, Relative tail current estimated by ratio of CA-sensitive current and current in control conditions. Tail currents were recorded on repolarization to −60 mV after 5-second pulses to 0 mV. Points are mean and lines SEM of 11 experiments.

−120 to −60 mV after a 500-ms pulse to +50 mV. Representative examples of the time course of recovery from inactivation and its fitting to a monoexponential process are shown in Figure 6E. The mean time constants for recovery from inactivation in the absence and the presence of CA were plotted against voltage in Figure 6F. CA did not modify the kinetics of the reactivation process at any of the potentials tested.

Effects of CA on Native I_{Kr}

Figure 6A shows the I_K recorded on isolated guinea-pig ventricular myocytes in the presence of 2 mmol/L Co^{2+}-containing solution. After 5 seconds of depolarization to +50 mV, the cell was repolarized at 0 mV for 10 seconds. Under these conditions, the I_{Ks} was deactivated, and hyperpolarization to −60 mV elicited a tail current, which is caused primarily by the I_{Kr} because of its marked inward rectifier properties. CA, 50 μmol/L, decreased the maximum and the tail current elicited by the first depolarizing pulse (36.2±4.6%, n=4) and the tail amplitude obtained at −60 mV (31.6±5.9%). Figure 6B shows that 0.1 μmol/L aldosterone decreased the maximum current elicited by the depolarization to +50 mV (22.0±3.6%) and the tail current on repolarization to −60 mV (13.5±2.1%, n=4). Addition of CA in the presence of aldosterone further decreased the maximum and the tail current elicited on repolarization to −60 mV (53.3±3.2%, n=4).

Discussion

Our results demonstrate for the first time that SP and its metabolite CA directly block HERG channels. It should be stressed that the experiments were carried out in the absence of aldosterone, and thus, the observed effects are not attributable to antagonism of its effects at the aldosterone receptor level. Furthermore, both CA and aldosterone blocked the native I_{Ks} and I_{Kr} currents, and the effects of CA on I_{Kr} were comparable to those produced on HERG currents.

The concentration-dependent effects of CA on HERG channels are unusual, and at a wide range of concentrations (0.01 to 1000 nmol/L), blockade was almost concentration-independent. The reason for this behavior is unknown, but it may be related to the anionic nature of both SP and CA. In

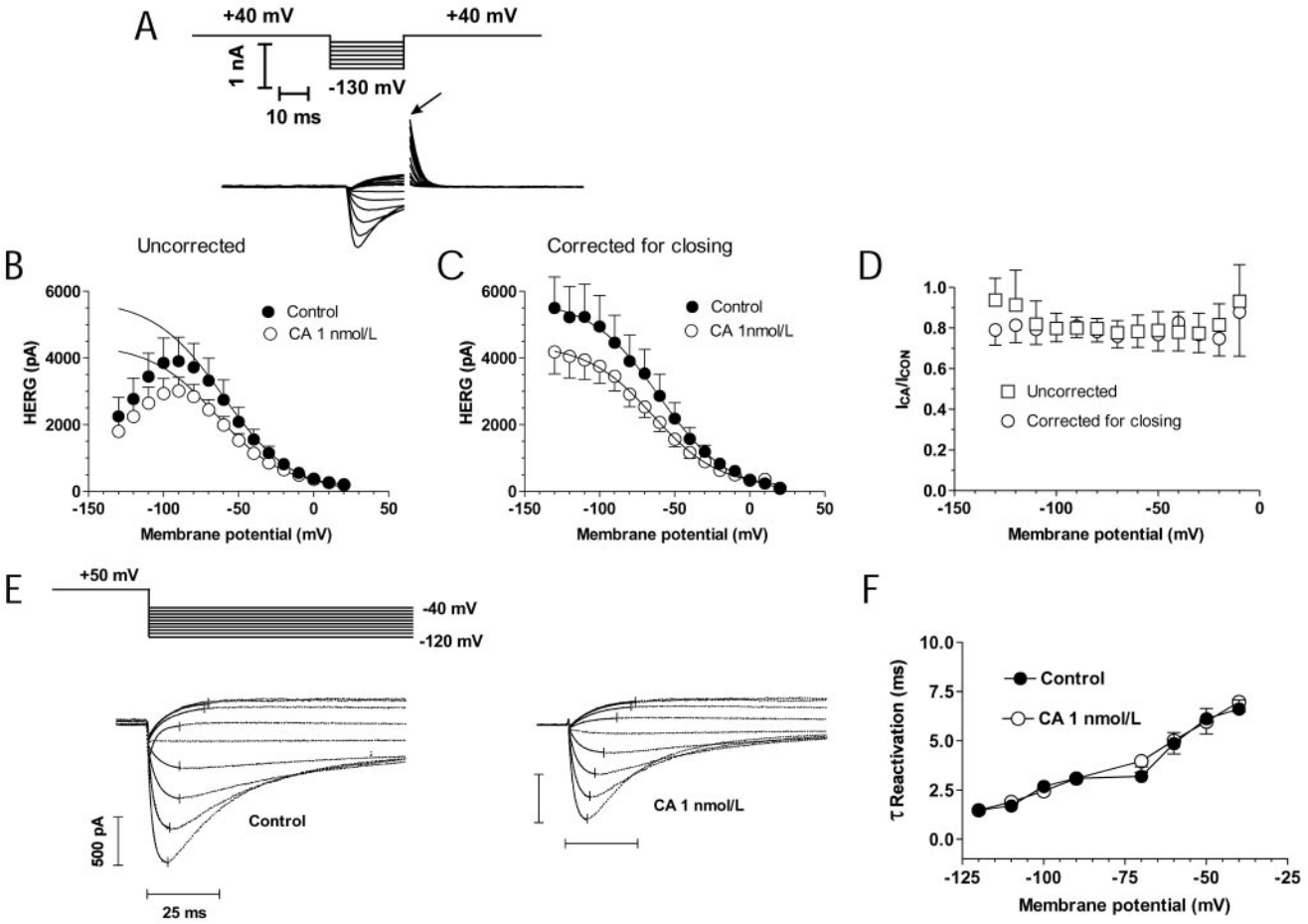

Figure 5. A, Current records obtained with protocol used to assess steady-state inactivation. After inactivation was allowed to relax to steady-state at potentials ranging from −130 to +20 mV during 20 ms, membrane voltage was stepped to +40 mV for 225 ms. B, Steady-state inactivation from A. Initial current (arrow in A) obtained in absence and in presence of 1 nmol/L CA was plotted as a function of previous voltage step. C, Corrected for closing inactivation curve obtained in presence and in absence of CA. D, Fractional block for both uncorrected and corrected for closing initial current amplitudes as a function of interpulse potential. E, Current traces recorded in absence and in presence of CA with protocol used to assess recovery from inactivation. Time course of recovery from inactivation was measured by fitting exponential functions (continuous lines) to tail currents elicited after repolarization from a 500-ms pulse to +50 mV from a holding potential of −80 mV. F, Mean time constant values of recovery of inactivation in control conditions and in presence of CA as a function of membrane potential. B through D and F, Points represent mean±SEM of 6 experiments.

fact, this is the first report of a concentration-dependent interaction between an anionic drug and the HERG channels. Further studies are necessary to elucidate whether only 1 molecule of CA binds to the pore cavity of the HERG channels to block the K^+ efflux.

The effects of CA on HERG channels were voltage- and frequency-independent, indicating that CA blocks HERG channels in the closed state or/and preferentially binds to the open state, with very fast kinetics of development of block. Results of the envelope of tail test suggested that blockade appeared before channels activated and that channel activation led to only a small increase in block. Conversely, at the beginning of the tail currents elicited on repolarization after pulses to 0 mV, a small increase of block was observed, and thereafter, as the closing progressed, the blockade decreased. Moreover, no time-dependent development of block was resolved when currents at 0 mV were recorded after strong and brief depolarizing pulses. All these results suggested that CA binds to a closed state (or active but not open) from which opening proceeds, as well as to the open state of the HERG channels. However, CA did not modify the voltage-dependence of inactivation or the time course of reactivation of HERG channels, which indicated that CA did not bind to the inactivate state of the channel.

SP also decreased HERG currents in a concentration-dependent manner, its effects being voltage-independent after HERG channel activation reached saturation. Because SP is metabolized too rapidly to be detected in plasma, no further effort was made to determine the possible state-dependence of the blockade observed.

Clinical Implications

After oral administration, SP is metabolized rapidly (half-life ≈1.5 hours), whereas its metabolites (canrenone and/or CA) have considerably longer half-life values (≈16.5 hours). Peak plasma concentration of canrenone after administration of therapeutic doses of SP range between 0.3 and 1.6 μmol/L. Canrenone is extensively (98%) bound to plasma proteins and

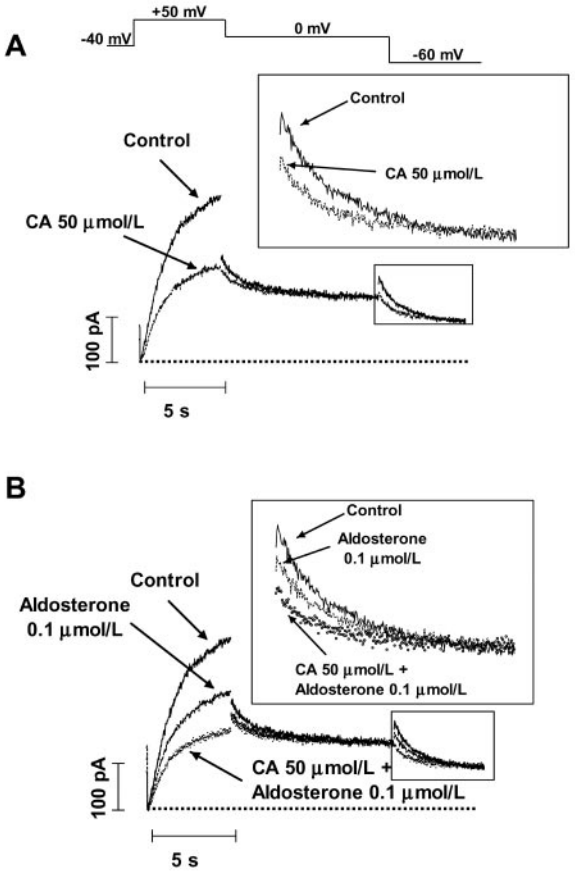

Figure 6. Effects of 50 μmol/L CA (A) and 0.1 μmol/L aldosterone alone and with CA (B) on I_K recorded in guinea pig ventricular myocytes when applying pulse protocol shown at top. Insets show tail currents elicited by hyperpolarization to −60 mV in an expanded scale. Dashed line represents zero current level.

is in enzymatic equilibrium with CA, producing peak free plasma concentrations of CA of 3 to 16 nmol/L.[5] Therefore, our study demonstrated that at concentrations within the therapeutic range, CA blocks HERG channels. As a consequence, a prolongation of the atrial and ventricular action potentials would be expected, an effect already described in multicellular preparations.[6,7] Prolongation of the duration of the cardiac action potential (APD) and refractoriness has been recognized as an antiarrhythmic effect. However, blockade of HERG channels can lead, under some circumstances, especially in the setting of hypokalemia, bradycardia, or both, to an excessive prolongation of the APD and of the QT interval. This latter effect is considered to be proarrhythmic, because it might produce polymorphic ventricular tachycardias known as torsades de pointes.[14] Conversely, SP antagonized the hypokalemia and hypomagnesemia produced by aldosterone, an effect that may blunt the blockade of HERG channels.[15] Furthermore, the blockade of Ca^{2+} channels produced by SP[16] would shorten the APD and suppress early afterdepolarizations. Therefore, further studies are needed to analyze the resultant effects of SP/CA on human cardiac repolarization and its possible clinical implications.

Acknowledgments

This work was supported by Comisión Interministerial de Ciencia y Tecnología (SAF99-0069/2002-02304), Comunidad Autónoma de Madrid (08.4/0038.1/2001), Fondo de Investigaciones Sanitarias (01/1130), the Spanish Society of Cardiology, and Pfizer Foundation Grants. We thank Dr M. Sanguinetti for his helpful comments and Drs S. Nattel, M. Weerapura, and T. Hebert for CHO cells stably expressing HERG.

References

1. Givertz M. Manipulation of the renin-angiotensin system. *Circulation*. 2001;104:e14–e18.
2. Pitt B, Zannad F, Remme W, et al. The effect of spironolactone on morbidity and mortality in patients with severe heart failure. *N Engl J Med*. 1999;341:709–717.
3. Yee K-M, Pringle S, Struthers A, et al. Circadian variation in the effects of aldosterone blockade on heart rate variability and QT dispersion in congestive heart failure. *J Am Coll Cardiol*. 2001;37:1800–1807.
4. Stier CT, Chander PN, Rocha R. Aldosterone as a mediator in cardiovascular injury. *Cardiol Rev*. 2002;10:97–107.
5. Karim A. Spironolactone: disposition, metabolism, pharmacodynamics, and bioavailability. *Drug Metab Rev*. 1978;8:151–188.
6. Briggs A, Holland W. Antifibrillatory effects of electrolyte regulating esteroids on isolated rabbit atria. *Am J Physiol*. 1959;197:1161–1164.
7. Coraboeuf E, Deroubaix E. Effect of a spirolactone derivative, sodium canrenoate, on mechanical and electrical activities of isolated rat myocardium. *J Pharmacol Exp Ther*. 1974;191:128–138.
8. Tseng G. I_{Kr}: the HERG channel. *J Mol Cell Cardiol*. 2001;33:835–849.
9. Weerapura M, Nattel S, Chartier D, et al. A comparison of currents carried by HERG, with and without coexpression of MiRP1, and the native rapid delayed rectifier current. *J Physiol (Lond)*. 2002;540:15–27.
10. Caballero R, Delpón E, Valenzuela C, et al. Losartan and its metabolite E3174 modify cardiac delayed rectifier K^+ currents. *Circulation*. 2000; 101:1199–1205.
11. Zhang S, Rajamani S, Chen Y, et al. Cocaine blocks HERG, but not KvLQT1+minK, potassium channels. *Mol Pharmacol*. 2001;59: 1069–1076.
12. Smith P, Baukrowitz T, Yellen G. The inward rectification mechanism of the HERG cardiac potassium channel. *Nature*. 1996;379:833–836.
13. Spector P, Curran M, Zou A, et al. Fast inactivation causes rectification of the I_{Kr} channel. *J Gen Physiol*. 1996;107:611–619.
14. Roden D. Mechanisms and management of proarrhythmia. *Am J Cardiol*. 1998;82:491–571.
15. Yang T, Roden D. Extracellular potassium modulation of drug block of I_{Kr}. *Circulation*. 1996;93:407–411.
16. Dacquet C, Loirand G, Mironneau C, et al. Spironolactone inhibition of contraction and calcium channels in rat portal vein. *Br J Pharmacol*. 1987;92:535–544.